Comparative Visualization Using Cross-Mesh Field Evaluations and Derived Quantities

Hank Childs[1], Sean Ahern[2], Jeremy Meredith[2], Mark Miller[3], and Kenneth I. Joy[4]

1   Lawrence Berkeley National Laboratory Berkeley, California, USA hchilds@lbl.gov

2   Oak Ridge National Laboratory Oak Ridge, Tennessee, USA ahern@ornl.gov

3   Lawrence Livermore National Laboratory Livermore, California, USA miller86@llnl.gov

4   Institute for Data Analysis and Visualization Computer Science Department University of California Davis, California, USA joy@cs.ucdavis.edu

Comparative Visualization Using Cross-Mesh Field Evaluations and Derived Quantities

Hank Childs[1], Sean Ahern[2], Jeremy Meredith[2], Mark Miller[3], and Kenneth I. Joy[4]

1   **Lawrence Berkeley National Laboratory**
    Berkeley, California, USA
    `hchilds@lbl.gov`
2   **Oak Ridge National Laboratory**
    Oak Ridge, Tennessee, USA
    `ahern@ornl.gov`
3   **Lawrence Livermore National Laboratory**
    Livermore, California, USA
    `miller86@llnl.gov`
4   **Institute for Data Analysis and Visualization**
    Computer Science Department
    University of California
    Davis, California, USA
    `joy@cs.ucdavis.edu`

—— Abstract ——

We present a data-level comparative visualization system that utilizes two key pieces of technology: (1) cross-mesh field evaluation – algorithms to evaluate a field from one mesh onto another – and (2) a highly flexible system for creating new derived quantities. In contrast to previous comparative visualization efforts, which focused on "$A - B$" comparisons, our system is able to compare many related simulations in a single analysis. Types of possible novel comparisons include comparisons of ensembles of data generated through parameter studies, or comparisons of time-varying data. All portions of the system have been parallelized and our results are applicable to petascale data sets.

1   Introduction

One of the most common activities of an analyst is to perform comparisons. These comparisons take different forms: comparing a simulation to experimental data, comparing a simulation to a legacy simulation result, comparing the results of a simulation before and after key algorithmic changes, comparing the results of two simulations with different initial geometries. These are generally "A-B" type comparisons, where two results are compared. Sometimes, however, the comparisons need to take place between a series of data sets, for example when doing a parameter study or looking at time-varying data.

In this paper, we present a powerful system for facilitating data-level comparisons. Our system incorporates multiple inputs and creates an output data set that reflects a comparison. The system combines two key technologies:

1. *cross-mesh field evaluation* (CMFE), where a field from a "donor" mesh is evaluated onto a "target" mesh, and
2. *derived quantity generation*, where new fields are created from existing ones

These two capabilities combine to form a powerful and flexible system where end users are given great latitude to create data sets tailored to application specific comparative metrics.

Given a set of donor meshes $M_1, M_2, ..., M_k$ each containing a corresponding field $F_1, F_2, ..., F_k$, and a target mesh M_C, We evaluate each field F_i onto M_C, creating a new field on the target mesh.

These new fields are analyzed using the derived quantity subsystem, creating a new field over M_C that can be displayed using conventional visualization methods. Cross-mesh field evaluation is related to derived quantity generation because, from the perspective of the target mesh, it results in the creation of a new field. We exploit this relationship by integrating cross-mesh field evaluation with derived function generation in a data-parallel distributed memory implementation, making it applicable to a number of very large scale problems.

Research related to this effort is addressed in Section 2. Section 3 describes data-level comparison methods and illustrates the problems of cross-mesh field evaluation. Section 4 describes our system and the data-parallel implementation of cross-mesh field evaluation. Results of this effort are given in Section 5, and in the supplementary material.

2   Related Work

Three basic areas of comparative visualization – *image-based*, *data-level*, and *topological* comparisons – have been discussed in the literature (see Shen et al. [17]). Image-based methods generate multiple images, and provide methods by which a user can compare the image data; data-level methods compare the actual data between input data sets, and provide methods by which the differences can be compared; and topological-based methods compare results of features generated for each of the input data sets.

Most image-based comparison systems [9, 21, 22] perform image differencing algorithms on images from multiple inputs. These systems are limited to comparing visualizations where the data set can be represented by a single image. These techniques are extremely important in the context of comparison to experimental results, such as in the case with [9] and [22]. The VisTrails system of Bavoil et al. [3] coined the phrase *multiple-view comparative system* to describe image-based systems where plots are placed side-by-side or potentially overlaid. In multiple-view comparative systems, the burden is placed on the human viewer to visually correlate features and detect differences.

Topological methods [2, 10, 20] compare features of data sets. Typically, they survey the data set, create summaries of the data, and develop image-based or data-level methods to visualize these summaries.

The ALICE Differencing Engine of Freitag and Urness [11] is a data-level comparison tool. It is limited to comparing data sets that have identical underlying meshes and only allows data differencing comparisons. Shen et al. [17, 18] place data sets on an target mesh and utilize derived quantities to form comparisons. Sommer and Ertl [19] also base their comparisons on data-level methods. Their system employs only connectivity-based differencing, although they also consider the problem of comparisons across parameter studies.

Many visualization systems [1, 7, 12] provide subsystems for generating derived quantities. Moran and Henze give an excellent overview in [15] of their DDV system, using a demand driven calculation of derived quantities. McCormick et al. furthered this approach with Scout [14] by pushing derived quantity generation onto the GPU. Joy et al. [13] have developed statistics-based derived quantities that greatly expand the uses of derived functions.

Our comparative visualization system has been deployed within VisIt [6], an open source visualization system designed to support extremely large scale data sets. As with many visualization tools [12, 1], it has a data flow network design that leverages pieces of VTK [16]. A key differentiating aspect is its strong contract basis [5], which enables many algorithms to be implemented in parallel. As with the system of Shen et al. [17, 18], the data sets to be compared are placed on a target mesh and derived quantities are generated. Our system contains the following extensions:

- comparison of more than two input data sets, which enables powerful applications for time-varying data and parameter studies,
- the flexibility of applying either position-based or connectivity-based comparisons, and
- a fully parallel, distributed memory solution.

3   Data-level Comparison Methods

Let $M_1, M_2, ..., M_k$ denote a set of donor meshes, each containing a corresponding field $F_1, F_2, ..., F_k$, and let M_C denote some target mesh. The cross-mesh evaluation step evaluates each field F_i, for $i = 1, ..., k$, onto M_C, creating new fields $F_{C,i}, i = 1, ..., k$ that represent each of the original fields on the target mesh. We then employ a function, $D(F_{C,1}, F_{C,2}, ..., F_{C,k}) \rightarrow \Re$, that takes elements of the k fields as input and produces a new derived quantity. The resulting field F_D, defined over M_C, is then visualized with conventional algorithms. (Most previous systems consider only M_1 and M_2 and visualize $F_D = F_{C,1}$ - $F_{C,2}$.)

M_i and F_i can come from simulation or experimental observation. Some common examples are: two or more related simulations at the same time slice, multiple time slices from one simulation, or a data set to be compared with an analytic function.

The target mesh M_C can be a new mesh or one of the donor meshes M_i. In practice, we frequently use the latter option. However, this system supports the generation of new arbitrary rectilinear grids with a user-specified region and resolution.

There are two choices for generating $F_{C,i}$: the evaluation can be made either in a position-based fashion or in a connectivity-based fashion. *Position-based evaluation* is the most common method. Here, the donor and target meshes are overlaid and overlapping elements (cells) from the meshes are identified. Interpolation methods are applied to evaluate F_i on M_C. This technique is difficult to implement, especially in a parallel, distributed memory setting, because M_C and M_i may be partitioned over processors differently – which requires a re-partitioning to align the data. This re-partitioning must be carefully constructed to ensure that no processor exceeds primary memory.

Connectivity-based evaluation requires that both the donor mesh, M_i, and the target mesh, M_C, are *homeomorphic*. That is, they have the same number of elements and nodes, and the element-to-node connectivities for all elements are the same. This is often the case if M_C is selected from one of the M_i, because for comparisons across time and/or parameter studies the remaining $M_{j:j\neq i}$ typically have the same underlying mesh. In this case, the value of an element or node in M_i is directly transferred to the corresponding element or node in M_C. Connectivity-based cross-mesh field evaluation is substantially faster; the difficult task of finding the overlap between elements is eliminated.

For Eulerian simulations (where node positions are constant, but materials are allowed to move through the mesh), connectivity-based evaluation yields the same results as position-based evaluation but with higher performance. For Lagrangian simulations (where materials are fixed to elements, but the nodes are allowed to move spatially), position-based evaluations are used most often, because connectivity-based evaluations typically do not make sense in the context of moving nodes. However, connectivity-based evaluation allows for new types of comparisons, because comparisons can take place along material boundaries, even if they are at different spatial positions. Further, connectivity-based evaluations allow for simulation code developers to pose questions such as: how much compression has an element undergone? (This is the volume of an element at the initial time divided its volume at current time.)

There are limitless forms of derived quantities, F_D, that are necessary for different types of comparisons in different situations. We list a few of the most frequently used in Table 1 as examples.

	Description	Definition
1	Difference	$F_2 - F_1$
2	Relative difference	$(F_2 - F_1)/(F_2 + F_1)$
3	Maximum or minimum	$(F_2 > F_1 ~?~ F_2 : F_1)$
		$(F_2 < F_1 ~?~ F_2 : F_1)$
4	Determine the simulation containing the maximum or minimum	$(F_2 > F_1 ~?~ 2 : 1)$
		$(F_2 < F_1 ~?~ 2 : 1)$
5	Average	$(F_2 + F_1)/2$

■ **Table 1** Common derived quantities for comparisons. For simplicity, we assume only two donor meshes, M_1 and M_2. The target mesh (M_C) is M_2, and the fields from the evaluation phase are F_1 and F_2. Derivation 1 allows users to explore the differences between the two data sets. Derivation 2 is used in a similar fashion, but amplifies small changes on relatively small quantities. Derivations 3-5 (minima, maxima, and averages) are useful when going beyond simple "$A - B$" comparisons for a large number of donor meshes. When analyzing time series or parameter studies with many related inputs, these quantities allow for visualization of all data sets with a single, composite data set.

4   System Description

Three critical pieces make up the comparative system: the derived quantity system, the cross-mesh field evaluation methods, and key portions that allow a distributed, parallelized implementation. We describe our comparative system within the constraints of VisIt [6].

4.1   Data-flow-based Visualization Systems

A number of visualization systems make heavy use of data flow networks, a common design for providing interoperability and extensibility. An instantiation of a data flow network, referred to as a pipeline, consists of a source, filters, and a sink. An example source is a file reader, an example sink is a rendering module, and an example filter is a visualization algorithm, such as slicing or contouring. In this model, data flows from the source, through the filters, and ultimately to the sink.

When operating in parallel, each of VisIt's processors instantiate an identical data flow network, which only differs in the data it operates on. So, when each filter executes, there are multiple instances of this filter, one on each processor, and the inputs to these filters form a partition of the input data set.

4.2   Derived Quantities

There are two key areas to VisIt's derived quantity system. One is the expression language that allows end users to create new, arbitrary derived quantities. The other is the mechanism that transforms an instance of an expression into a form suitable for data flow networks.

4.2.1   Expression Language

We have developed a functional, string-based system to allow users to create new derived quantities. This results in an expression language syntax that enables users to compose derived quantities in arbitrary ways. A major goal of the design of our expression language was to provide an intuitive interface where creation of new derived quantities required little to no learning curve for common operations. For example, the average of two fields, A and B, is as simple as "(A+B)/2".

Of course, users will want to create derived quantities that are more than simple mathematical constructs. Support exists in the language for composing scalar quantities into vectors or tensors, and for extracting scalar components back out. Notation for strings, lists, ranges, and strides allows selection of materials, parts, and other subsets of elements. For accessing other files, either within the same sequence or in different sequences, the language supports references by cycle, absolute and relative time index, and filename. Other named operations are referenced as functions, and a small selection of the over one hundred available are listed in table 2.

■ **Table 2** Our expression language allows for all of these functions to be combined in arbitrary ways.

Math	+, -, *, /, power, log, log10, absval, ...
Vector	cross, dot, magnitude
Tensor	determinant, eigenvector, effective (e.g. strain), ...
Mesh	coordinates, polar, volume, area, element_id, ...
Field Operator	gradient, divergence, curl, Laplacian
Relational	if-then-else, and, or, not, $<, \leq, >, \geq, =, \neq$
Mesh Quality	shear, skew, jacobian, oddy, largest angle, ...
Trigonometric	sine, cosine,..., arctangent, degree2radian, ...
Image Filters	mean, median, conservative smoothing
Miscellaneous	recenter, surf. normal, material vol. fraction, ...

The strength of our expression language lies in the richness of functionality and the interoperability between these expressions. Consider, for example, computing divergence ($\triangledown$). If a two-dimensional vector F is defined as $P\hat{x} + Q\hat{y}$, then $\triangledown F = \frac{\partial P}{\partial x} + \frac{\partial Q}{\partial y}$. A user can calculate divergence directly using the built-in function, divergence(). But, for illustrative purposes, it is also straightforward to calculate divergence using other functions as building blocks: "divF = gradient(P)[0] + gradient(Q)[1]". VisIt has a custom scanner and parser that constructs a parse tree based on expressions like this one. Figure 1 contains the parse tree for this divergence expression.
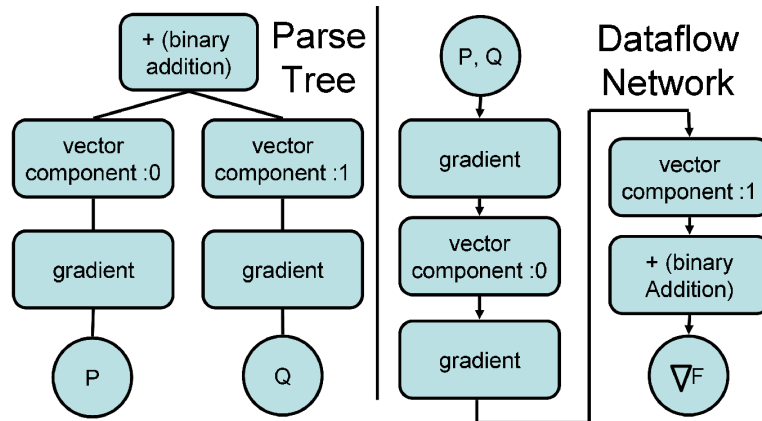
■ **Figure 1** Creation of a derived quantity. On the left, we see an expression's parse tree. On the right, we see the linearized data flow network for that parse tree.

When VisIt assembles a data flow network, it relies on an Expression Evaluator Filter (EEF) to construct derived quantities. The EEF is typically inserted as the first filter in the pipeline, immediately following the file reader module. In a preparatory phase, the other filters place the names of

their required variables into a list. When executing, the EEF cross-references this list with known expression names to determine what derived quantities need to be calculated.

The EEF dynamically creates a sub-network to create needed derived quantities. To do this, it first consults the parse trees of the expressions. For each node in each parse tree, a filter that can perform the corresponding operation is placed into the sub-network. Ultimately, this sub-network reflects a linearized form of the parse trees. The linearization process requires the EEF to do dependency checking between all of the parse trees for all of the expressions involved to ensure that every filter has the inputs it needs. VisIt's implementation supports the linearization of *any* parse tree, including this dependency checking.

Our system supports the accumulation of partial results onto the target mesh M_C so that individual $F_{C,i}$'s can be quickly discarded. While the sub-network is executing, the EEF is able to determine when intermediate variables are no longer needed and remove them. Through this mechanism, the EEF is able to successfully handle many related data sets that would otherwise exceed the available memory.

To perform a cross-mesh field evaluation, the user defines an expression involving built-in functions for the evaluation algorithms – position-based or connectivity-based. Like all other expressions, the comparison expressions have corresponding filters that can be placed in the sub-network to perform the cross-mesh evaluation. By combining these algorithms with expressions, users can direct the creation of new, derived quantities from a multitude of sources on the same target mesh. Furthermore, they can manipulate these quantities using all of the previously mentioned expressions to create interesting comparisons.

Finally, although derived quantity generation typically takes place immediately after reading the data, it is also possible to defer their evaluation until later in the pipeline. This ability allows for the target mesh to be transformed before the cross-mesh field evaluation takes place. This is important when registration is needed, for example for comparison with experimental data.

4.3   Cross-Mesh Field Evaluation

The implementations of the various filters for cross-mesh field evaluation (CMFE) are similar. They all have one input for the target mesh and they all are capable of dynamically instantiating an additional data flow network to obtain M_i and F_i. The differentiating point between the CMFE filters is how they evaluate the fields.

The connectivity-based CMFE algorithm is straightforward. For each element or node, it places F_i onto M_C to create $F_{C,i}$. The only subtlety is guaranteeing that the partitioning of the input data (in a parallel setting) is done so that each processor operates on the same chunks of data.

The position-based CMFE algorithm is complex. There are three major challenges:

1. the overlay step – identifying which elements of the donor mesh M_i overlap with an element in the target mesh M_C.
2. the interpolation step – fitting an interpolant for the field on the target mesh M_C such that it matches, as closely as possible, at key points on the donor mesh M_i.
3. Managing the distribution of data to maximize parallel computational efficiency in a distributed-memory environment.

4.3.1   The Overlay Step

We use interval trees [8] to efficiently identify elements from meshes M_i and M_C that overlap spatially. We start by placing all elements from M_i into the interval tree. Then, for each element of M_C, we use its bounding box to index the interval tree and find the list of elements from M_i with overlapping bounding boxes. We examine this list to find the elements that truly overlap (as opposed to only

having overlapping bounding boxes). If M_C contains N_C elements and M_i contains N_i elements, then the time to generate the tree is $O(N_i\log(N_i))$ and the time to locate the elements of M_i that overlap with an element of M_C is $O(\log(N_i) + \alpha)$, where α is the number of elements from M_i returned by the search. This gives a total time of $O((N_C + N_i)*\log(N_i))$. Note that α is amortized out for all but degenerate mesh configurations.

4.3.2   Field Interpolation

For each position x on the target mesh M_C, we evaluate the field on the donor mesh M_i at x, and assign the value at that location to M_C. This method was chosen because it favors performance over accuracy. A good improvement to our implementation, however, would be to add the use of weighted averaging with weights based on volume overlaps.

4.3.3   Parallel Implementation

The final piece of the problem is to perform cross-mesh field evaluations in a parallel, distributed-memory environment. The key issue deals with spatial overlap. When a processor is evaluating a field from mesh M_i onto the target mesh M_C, it must have access to the portion of M_i that overlaps spatially with the portion of M_C it is operating on. Our strategy for this issue is to create a spatial partition to guide re-distribution of both meshes for the evaluation phase. Unfortunately, the spatial partition must be created with great care. If the partition divides space into regions that cover appreciably different numbers of elements, it will lead to load imbalances and potentially exhaust memory. Therefore, we focus on creating a *balanced spatial partitioning*, where "balanced" implies that every region contains approximately the same number of elements, E_t (see Figure 2). The E_t elements from each region may contain different proportions of elements from M_C and M_i; in general, it is not possible to have this proportion be fixed and E_t be equal on all processors.
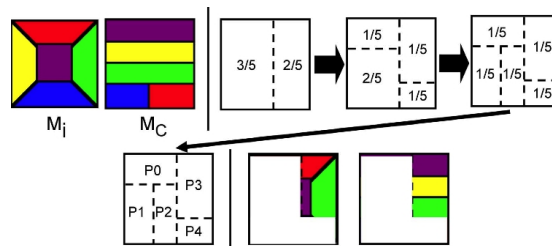
■ **Figure 2** In the upper left, two meshes, M_i and M_C, are shown. Assume the red portions are on processor 1, blue on 2, and so on. We employ an iterative strategy that creates a balanced spatial partition. We start by dividing in X, then in Y, and continue until every region contains approximately $1/N^{th}$ of the data, where N is the total number of processors. Each processor is then assigned one region from the partition and we communicate the data so that every processor contains all data for its region. The data for processor 3 is shown in the last set of figures.

The algorithm to efficiently determine a balanced spatial partitioning is recursive. We start by creating a region that spans the entire data set. On each iteration and for each region that represents more than $1/N^{th}$ of the data (measured in number of elements covered), we try to select "pivots", possible locations to split a region along a given axis. This axis changes on each iteration. All elements are then traversed, and their positions with respect to the pivots are categorized. If a pivot exists that allows for a good split, then the region is split into two sub-regions and recursive processing continues. Otherwise we choose a new set of pivots, whose choice incorporates the closest matching pivots from the previous iteration as extrema. If a good pivot is not found after

some number of iterations, we use the best encountered pivot and accept the potential for load imbalance.

The implementation of this algorithm is complicated by doing many parallel pivot locations at one time. The above procedure, if performed on a single region at a time, would have a running time proportional to the number of processors involved, which is unacceptable. To overcome this, we concurrently operate on many regions at one time. When iterating over a list of elements, we avoid the poor strategy of interacting with regions that do not even contain the element. Instead, we employ a separate interval tree that stores the bounding boxes of the regions. Then, for each element, we can quickly locate exactly the regions that element spans. This variation in the algorithm gives a running time proportional to the logarithm of the number of processors, which is more palatable.

Balanced spatial partitioning only guarantees that the total number of elements from both M_C and M_i are approximately equal. Our interval tree-based approach gives the best results if the number of elements from M_i are balanced as well.

After the best partition is computed, we create a one-to-one correspondence between the regions of that partition and the processors. We then re-distribute M_i, F_i, and M_C with a large, parallel, all-to-all communication phase. If elements belong to multiple regions, they are sent to all corresponding processors. After the communication takes place, evaluation takes place using the interval-tree based identification method described previously. Finally, all of the evaluations are sent back to the originating processor and placed on M_C.

We used the data set from Section 5 for a rough illustration of performance. The evaluation is of a 1.5 million element unstructured grid onto a 1K x 1K x 676 rectilinear grid, in parallel, using eighty processors. The most expensive phase is evaluation. In this phase, each processor is doing nearly ten million lookups on its interval tree. Table 3 summarizes the times spent in different phases of the algorithm. The inclusion of this information clearly does not serve as a performance study, which will be studied further in the future. However, it does inform as to the general running time for large problems.

Phase	Create Spatial Partition	Communi-cation of Data	Build Interval Tree	Eval
Time	0.7s	2.9s	5.2s	27.4s

■ **Table 3** The time spent in the different phases of the parallelized cross-mesh field evaluation algorithm. The communication column represents communicating data to create the balanced spatial partitioning, and also the time to return the final evaluations.

5   Results

We have provided an interface that allows the user to manage the entire comparison process, including what data sets are compared, how, and onto what target mesh. This system has been implemented in VisIt. We illustrate the systems use through the following examples.

### 5.1   Rayleigh-Taylor Instabilities

Rayleigh-Taylor instability simulations model the mixing of heavy and light fluids. For this study, we looked at two types of related data sets. First, we investigated a single simulation and its evolution in time. Then we looked at a parameter study, where turbulence parameters were varied to study how differences in these parameters affected the results.

5.1.1   Time-Varying Data

We started our analysis by looking at a single Rayleigh-Taylor instability calculation that simulated ten microseconds, outputting eighty-five time slices. Rather than focus on the differences between two time slices, we created visualizations that would summarize the whole data set. In particular, we were interested in summaries derived from a given binary condition, $B_C(P, T)$, where $B_C(P, T)$ is true if and only if condition C is true at point P and time T. For a given point P, the derived quantity was:

$$time(P) : B_C(P, time) \text{ AND } (\neg \exists t' : t' < time \text{ AND } B_C(P, t'))$$

This derived quantity is a scalar field that, for each point P, represents the first time that $B_C(P, T)$ is true. For our study, since we were observing the mixing of two fluids, we chose $B_C(P, T)$ to be whether or not mixing between the fluids occurs at point P at time T. From Figure 3, we can see that the mixing rate increased as the simulation went on (because there is more red than blue in the picture). We comment that the technique demonstrated here, showing a plot of the first time a binary condition is true in the context of time varying data, is very general. Further, we believe this is the first time that it has been presented in the context of creating these plots of this form (by using of data-level comparative techniques).
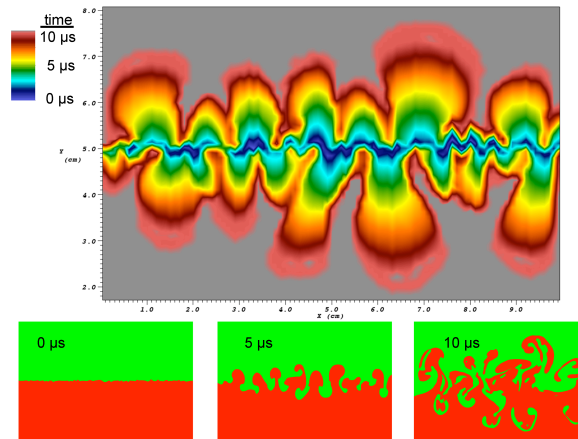
Figure 3 Along the top, we see a visualization comprising all time slices. Blue areas mixed early in the simulation, while red areas mixed later. Gray areas did not mix during the simulation. This plot allows us to observe mixing rates as well. Along the bottom, we include three time slices for reference. Heavy fluids are colored green, light fluids are colored red.

5.1.2   Parameter Studies

A simulation of a Rayleigh-Taylor instability is dependent on certain coefficients, which are adjusted in different situations. An important question is to understand how variation in these coefficients affects the outcome of a simulation. These effects can be monitored during parameter studies, where these coefficients are varied and the results are compared. For this parameter study, two coefficients were varied independently: the coefficient for turbulent viscosity and the coefficient of buoyancy. For each coefficient, five values were chosen. Twenty-five calculations were then performed, one for each pair of coefficients.

We focused on differences in magnitude of velocity, i.e. speed. This quantity had the most variation throughout the simulations and we wanted to characterize the relation between speed and the coefficients. We examined three different derived quantities defined over the whole mesh. The first

quantity was the simulation index that resulted in the maximum speed at the given point. The second and third, respectively, were the coefficients of turbulent viscosity and buoyancy corresponding to that simulation index.

If i is a simulation identifier/index, $C_{tv}(S)$ and $C_b(S)$ are the turbulent viscosity and buoyancy coefficients for i, then the derived quantities, for each point P are:

1. $maxsid(P) = \underset{i \in 1,\ldots,25}{\arg\max} \, speed_i(\mathrm{P})$

2. $C_{tv}\_of\_max\_speed(P) = C_{tv}(maxsid(P))$

3. $C_b\_of\_max\_speed(P) = C_b(maxsid(P))$

The results of these derived quantities are displayed in Figure 4. From the $maxsid(P)$ plot, we can see that no one simulation dominates the others in terms of maximum speed. From the $C_b\_of\_max\_speed(P)$ plot, we can draw modest conclusions, but it would be difficult to claim that this term is greatly affecting which simulations have the maximum speed. From the $C_{tv}\_of\_max\_speed(P)$ plot, we can see that most of the high speeds either come from very low or very high turbulent viscosity coefficients (colored blue and red, respectively). We quantified this observation (see Table 4), and found that the simulations with extreme turbulent viscosity coefficients had over three quarters of the total area, meaning that the relationship between high speeds and turbulent viscosity is large.
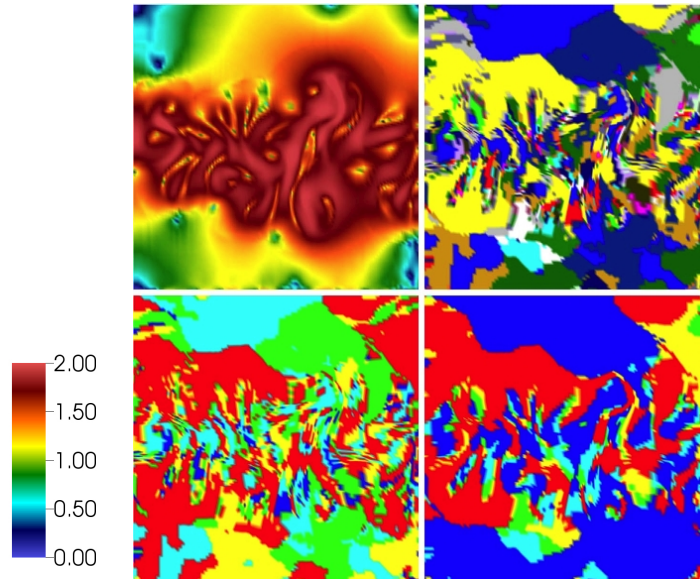
Figure 4 In the upper left, we see a normal rendering of speed for a single simulation. In the upper right, we color by $maxsid(P)$. In the lower left, we color by $C_b\_of\_max\_speed(P)$. In the lower right, we color by $C_{tv}\_of\_max\_speed(P)$.

Coefficient	very low	low	middle	high	very high
Buoyancy	4.2%	21.1%	20.4%	17.5%	36.8%
Turbulent Viscosity	47.2%	8.1%	4.8%	8.7%	31.0%

Table 4 Quantifying how much space each coefficient covered in terms of percentage of the total space.

Finally, we were also interested in quantifying the changes from simulation to simulation in our parameter study. We did this by calculating the following derived quantities:

1. $\frac{1}{25}\sum_{i=1}^{25} speed_i$ 2. $\max\limits_{i=1,...,25} speed_i$

3. $\min\limits_{i=1,...,25} speed_i$ 4. $\max\limits_{i=1,...,25} speed_i - \min\limits_{i=1,...,25} speed_i$

The results are shown in Figure 5. The fourth quantity informs an analyst as to the maximum differences possible for each point in space. Since we are performing these operations on a parameter study, we are effectively quantifying the uncertainty for this simulation. Of course, there are many alternative ways that an analyst may want to construct uncertainty information from ensembles of simulations. But we believe that through the examples we have presented in this section, we have motivated the capability of our system to do so and the importance of a flexible and powerful derived quantity system.
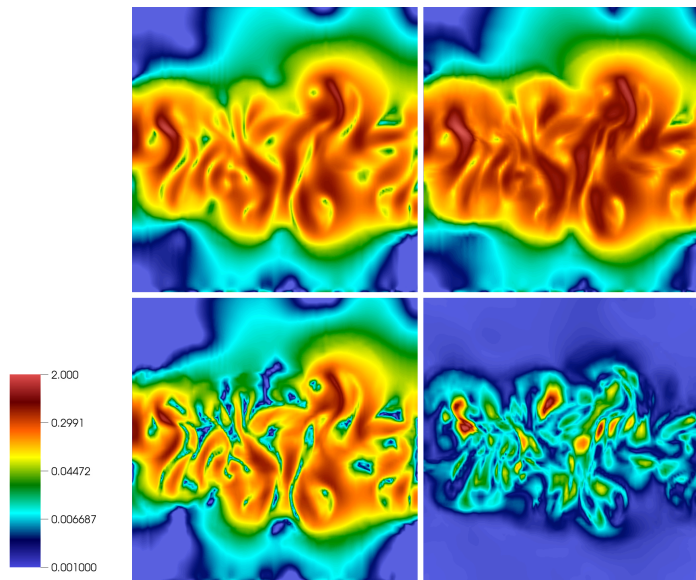
■ **Figure 5** In the upper left, we are coloring by average speed, in the upper right by maximum speed, in the lower left by minimum speed, and in the lower right maximum variation. The first three plots vary in speed from zero to two and are colored using a logarithmic scale. The fourth plot (of differences) ranges from zero to one and is colored linearly. These plots effectively quantify the uncertainty for this ensemble of simulations.

6   Conclusions

We have demonstrated a powerful system for data-level comparative visualization and analysis. The system we have developed supports a wide range of comparative analyses. In addition, the system is very versatile not only in the modalities of cross-mesh field evaluation it offers, but also in the range of derived quantities that can be generated. Finally, it supports these operations in a highly scalable, distributed memory, parallel computational paradigm.

This methodology has greatly expanded the types of comparative visualization that can be addressed. By integrating this system into an open-source product, we have been able to get this

technology in the hands of scientists and engineers. Future work will focus on the enhancements of these technologies to generate new comparative methods that impact their work.

───── **References** ─────────────────────────────────────

1 Greg Abram and Lloyd A. Treinish. An extended data-flow architecture for data analysis and visualization. Research report RC 20001 (88338), IBM T. J. Watson Research Center, Yorktown Heights, NY, February 1995.

2 Rajesh K. Batra and Lambertus Hesselink. Feature comparisons of 3-D vector fields using earth mover's distance. In *Proceedings of the IEEE Visualization Conference*, pages 105–114, 1999.

3 L. Bavoil, S.P. Callahan, P.J. Crossno, J. Freire, C.E. Scheidegger, C.T. Silva, and H.T. Vo. Vis-Trails: enabling interactive multiple-view visualizations. *IEEE Transactions on Visualization and Computer Graphics*, 12(6):135–142, 2005.

4 Steven P. Callahan, Juliana Freire, Emanuele Santos, Carlos E. Scheidegger, Cláudio T. Silva, and Huy T. Vo. Vistrails: visualization meets data management. In *SIGMOD '06: Proceedings of the 2006 ACM SIGMOD international conference on Management of data*, pages 745–747, New York, NY, USA, 2006. ACM.

5 Hank Childs, Eric Brugger, Kathleen Bonnell, Jeremy Meredith, Mark Miller, Brad Whitlock, and Nelson Max. A contract based system for large data visualization. In *Proceedings of the IEEE Visualization Conference*, 2005.

6 Hank Childs and Mark Miller. Beyond meat grinders: An analysis framework addressing the scale and complexity of large data sets. In *SpringSim High Performance Computing Symposium (HPC 2006)*, pages 181–186, 2006.

7 Computational Engineering International, Inc. *EnSight User Manual*, May 2003.

8 T.H. Cormen, C.E. Leiserson, and R.L. Rivest. *Introduction to Algorithms*. McGraw-Hill Book Company, 1990.

9 Willem C. de Leeuw, Hans-Georg Pagendarm, Frits H. Post, and Birgit Walter. Visual simulation of experimental oil-flow visualization by spot noise images from numerical flow simulation. In *Visualization in Scientific Computing*, pages 135–148, 1995.

10 Herbert Edelsbrunner, John Harer, Vijay Natarajan, and Valerio Pascucci. Local and global comparison of continuous functions. In *Proceedings of the IEEE Visualization Conference*, pages 275–280, October 2004.

11 L. Freitag and T. Urness. Analyzing industrial furnace efficiency using comparative visualization in a virtual reality environment. Technical Report ANL/MCS-P744-0299, Argonne National Laboratory, 1999.

12 C.R. Johnson, S. Parker, and D. Weinstein. Large-scale computational science applications using the SCIRun problem solving environment. In *Proceedings of the 2000 ACM/IEEE conference on Supercomputing*, 2000.

13 Kenneth I. Joy, Mark Miller, Hank Childs, E. Wes Bethel, John Clyne, George Ostrouchov, and Sean Ahern. Frameworks for visualization at the extreme scale. In *Proceedings of SciDAC 2007, Journal of Physics: Conference Series*, volume 78, page 10pp, 2007.

14 Patrick S. McCormick, Jeff Inman, James P. Ahrens, Charles Hansen, and Greg Roth. Scout: A hardware-accelerated system for quantitatively driven visualization and analysis. In *Proceedings of the IEEE Visualization Conference*, pages 171–178, Washington, DC, 2004. IEEE Computer Society.

15 Patrick J. Moran and Chris Henze. Large field visualization with demand-driven calculation. In *Proceedings of the IEEE Visualization Conference*, pages 27–33, Los Alamitos, CA, 1999. IEEE Computer Society Press.

16 William J. Schroeder, Kenneth M. Martin, and William E. Lorensen. The design and implementation of an object-oriented toolkit for 3d graphics and visualization. In *Proceedings of the IEEE Visualization Conference*, pages 93–ff. IEEE Computer Society Press, 1996.

17 Qin Shen, Alex Pang, and Sam Uselton. Data level comparison of wind tunnel and computational fluid dynamics data. In *Proceedings of the IEEE Visualization Conference*, pages 415–418, Los Alamitos, CA, 1998. IEEE Computer Society Press.

18 Qin Shen, Sam Uselton, and Alex Pang. Comparison of wind tunnel experiments and computational fluid dynamics simulations. *Journal of Visualization*, 6(1):31–39, 2003.

19 O. Sommer and T. Ertl. Comparative visualization of instabilities in crash-worthiness simulations. In *Data Visualization 2001, Procceedings of EG/IEEE TCVG Symposium on Visualization*, pages 319–328, 2001.

20 Vivek Verma and Alex Pang. Comparative flow visualization. *IEEE Transactions on Visualization and Computer Graphics*, 10(6):609–624, 2004.

21 Peter L. Williams and Samual P. Uselton. Foundations for measuring volume rendering quality. Technical Report NAS/96-021, NASA Numerical Aerospace Simulation, 1996.

22 Hualin Zhou, Min Chen, and Mike F. Webster. Comparative evaluation of visualization and experimental results using image comparison metrics. In *Proceedings of the IEEE Visualization Conference*, Washington, DC, 2002. IEEE Computer Society.